N92-27732

A Six Degree-of-Freedom Magnetic Bearing for Microgravity Vibration Isolation *

A. Peter Allan and Carl R. Knospe
Department of Mechanical and Aerospace Engineering
University of Virginia

August 20, 1991

PRECEDING PAGE BLANK NOT FILMED

1 Introduction

The authors have previously presented a conceptual design for a coarse-fine actuator pair and discussed its efficacy in the microgravity vibration isolation application[1]. The coarse stage comprises a Stewart platform [2] which is mounted in a spacecraft and isolates low frequency, high amplitude vibrations. The fine stage is a novel magnetic bearing mounted on the Stewart platform (between the legs for compactness) and levitates the experiment to isolate all frequencies at low amplitudes. The combination is illustrated in Figure 1.

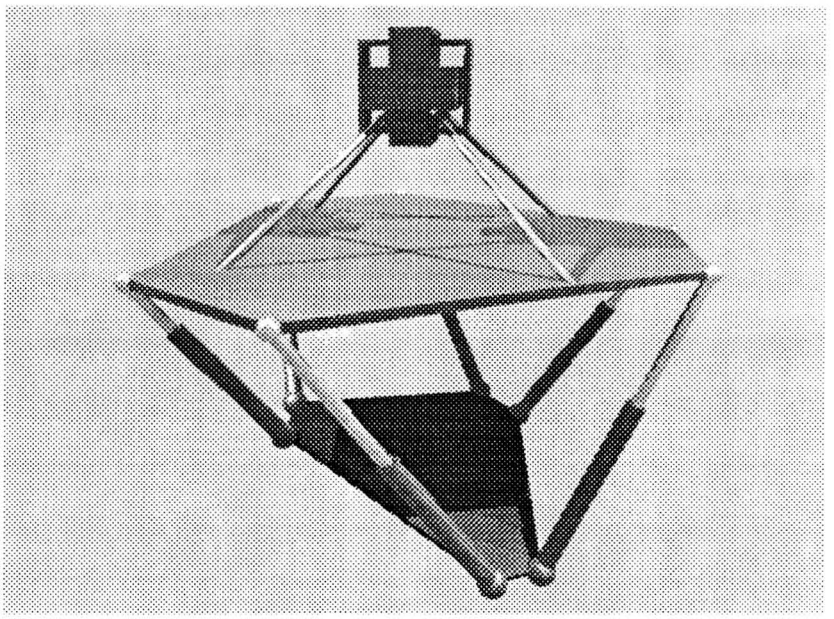

Figure 1: Coarse-Fine Actuator Pair

This paper will present a survey of published 6 DOF levitation designs and discuss a novel magnetic bearing in terms of design, predicted performance, and control issues.

*Supported in part by the NASA Lewis Research Center and the Commonwealth of Virginia's Center for Innovative Technology.

PRECEDING PAGE BLANK NOT FILMED

2 Survey of Published Designs

Several designs for 6 DOF levitation are discussed in the literature. A comparison of the specifications for these designs is given in Table 1.

Group	*Trans.*	*Rot.*	*Force*	*Envelope*	*Weight*	*Actuator*	*Sensor*
Honeywell	±5 mm	±1.6°	43 N	27x34x50 cm	36 kg	Mag. Brng.	Eddy & Flux
N. Wales	±5 mm	< ±.2°	.04 N [a]	100x100x100 cm [b]	?	Lorentz	Capacitive
NASA	±4 mm	±3° [c]	445 N	30x30x15 cm [c]	?	Mag. Brng.	Eddy
SatCon	±10 mm	±8° [c]	4 N	40x40x12 cm [c]	4.9 kg	Lorentz	Eddy
IBM	±5 mm	±4°	32 N	25x25x15 cm [c]	?	Lorentz	Optical
Toshiba	±2 mm	±1.5°	20 N [c]	25x25x20 cm	8 kg	Mag. Brng.	Eddy

[a] Requirement, not limitation
[b] Includes experiment package
[c] Estimated by authors

Table 1: Comparison of Published Designs

Four designs specifically for microgravity isolation have been published. Honeywell [3] has a well developed system called FEAMIS with which they have demonstrated impressive isolation performance. The system is designed for the Space Shuttle experiment configuration. The University College of North Wales [4] also has a well developed system designed for the European Space Agency experiment configuration. NASA [5] and SatCon [6] both have laboratory levitation systems.

Two levitation designs were developed for different applications, but they are mentioned here because they are similar and could be easily adapted to the isolation application. IBM [7] has a laboratory levitated robot "wrist" which enhances robot accuracy and performance. Toshiba [8] has a satellite antenna pointing system which is fully developed. Both devices have demonstrated positional accuracies on the order of 1 μm.

Isolation of vibrations with large amplitudes — typically occurring at low frequencies — requires a large translational range. SatCon's system has the largest range, but there is a significant tradeoff with the device's force capability. A coarse-fine approach would allow both a large range, provided by the coarse stage, and a high force capability, since the levitation gaps are small. There is no available data on the rotational range requirements of the application. Isolation with an umbilical disturbance requires a high force capability as is offered by the systems from Honeywell, NASA, IBM, and Toshiba. Space and weight should be minimized in any spacecraft. SatCon, IBM, and Toshiba's systems offfer advantages in envelope space and weight.

The choice of the actuator technology between Lorentz force and magnetic bearings has no definitive advantage. Lorentz actuators offer linearity, simplicity, and compactness. Magnetic bearings offer higher force capability and lower power consumption, particularly if gaps are minimized.

Four position sensor technologies offer promising performance. Eddy current position probes are simple and robust, but bulky and heavy for large gaps. Capacitive sensors are simple and light weight, but can be noisy in unconstrained environments. Optical lateral effect photo-diodes are compact and quiet, but they require substantial supporting electronics. Hall effect flux sensors can be used with magnetic bearing designs both to linearize the control problem, and to measure position.

3 Design

The magnetic bearing proposed has two parts: a stator which is attached to the spacecraft, and a surrounding "flotor" to which the experiment is attached.

The stator is illustrated in Figure 2. It has twelve pole pieces and coils arranged around the surface of a cube. The cube and pole pieces are ferromagnetic. Each pair of pole pieces and the region of the cube to which they are attached comprise a typical "horseshoe" electromagnet causing an attractive force toward the nearby flotor. Magnetic flux through the center of the cube will cause an imbalance in the flux levels of a pair of pole pieces, resulting in a net torque on the flotor. Differential Hall effect sensors will be located in the cube side of each pole piece to measure the local flux. All electrical connections will be to the stator.

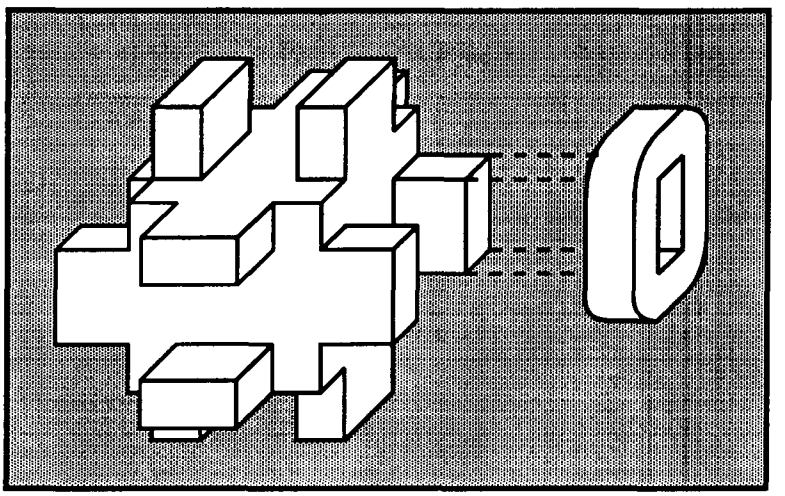

Figure 2: Stator and Typical Coil

The flotor is illustrated in Figure 3. Three ferromagnetic bands are rigidly attached to each other, but form independent flux paths. The bands are thicker in the region near the pole pieces to avoid saturation. Flux which passes through the center of the cube is returned through the remaining portion of the bands.

Four mounting posts will attach to corners of the cube, and pass through clearances in the flotor. These posts could carry cooling fluid to be circulated through the stator if it is required.

Design equations relating force and moments to the coil currents will be derived below referring to Figure 4. The figure shows a schematic slice through the stator and flotor with appropriate nomenclature and sign convention information. It should be noted that a complete model comprises three such systems, but they are identical and orthogonal, so only one will be analyzed.

The relationship between coil currents $(i_1, \ldots, i_4)$ and the force and moment generated in one slice of the stator (F_y, M_z) can be derived from Maxwell's Equations. The first Maxwell equation (1), which relates magnetic field intensity ($\underline{\mathrm{H}}$) around a closed path to the electric current density ($\underline{\mathrm{J}}$) through that path, is discretized and applied to closed loops drawn through the slice. N is the number of turns in each coil, and G_i are the air gap lengths which are dependent on the stator's position relative to the flotor. The iron flux paths are ignored because their reluctance is low relative to that of the air gaps. Many such equations can be written (2), but only three are independent.

$$\oint_C \underline{\mathrm{H}} \cdot d\underline{\mathrm{l}} = \int_S \underline{\mathrm{J}} \cdot d\underline{\mathrm{a}} \tag{1}$$

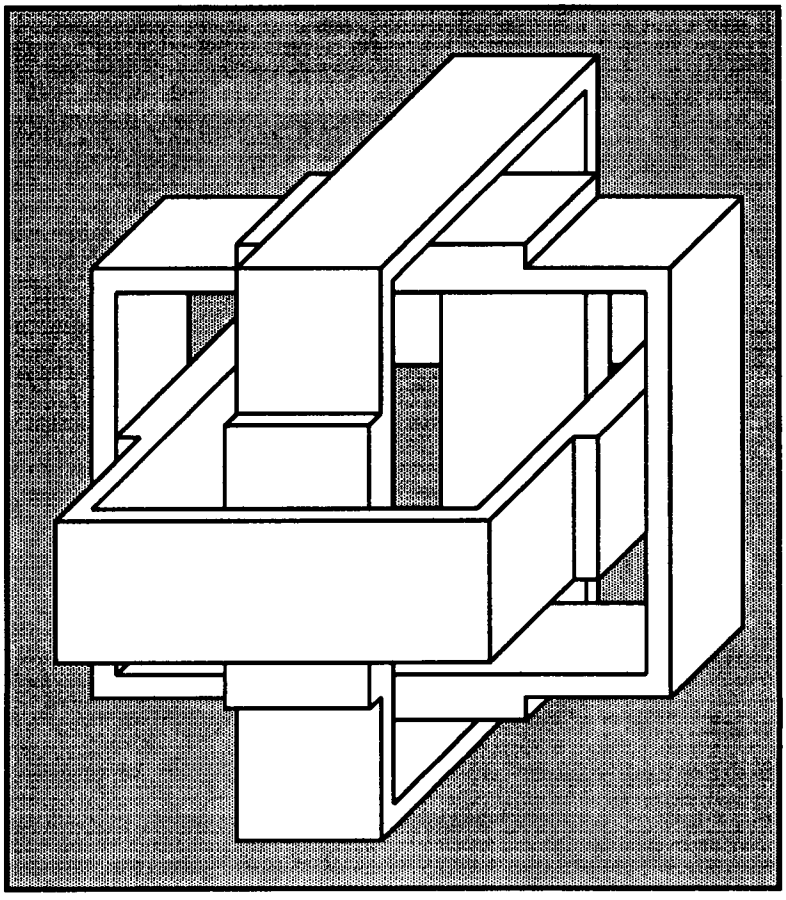

Figure 3: Flotor

$$\begin{aligned} H_1G_1 - H_2G_2 &= N(i_1 - i_2) \\ -H_3G_3 + H_4G_4 &= N(-i_3 + i_4) \\ -H_1G_1 - H_4G_4 &= N(-i_1 - i_4) \\ -H_2G_2 - H_3G_3 &= N(-i_2 - i_3) \\ &\vdots \end{aligned} \tag{2}$$

The second Maxwell equation (3), which ensures conservation of magnetic induction ($\underline{B}$), is used to obtain a fourth independent equation (4).

$$\underline{\nabla} \cdot \underline{B} = 0 \tag{3}$$

$$B_1 + B_2 - B_3 - B_4 = 0 \tag{4}$$

We can assume linear magnetization in the air gaps (5), where μ_0 is the permeability of free space, to obtain a relation between magnetic induction in the gaps and coil currents (6).

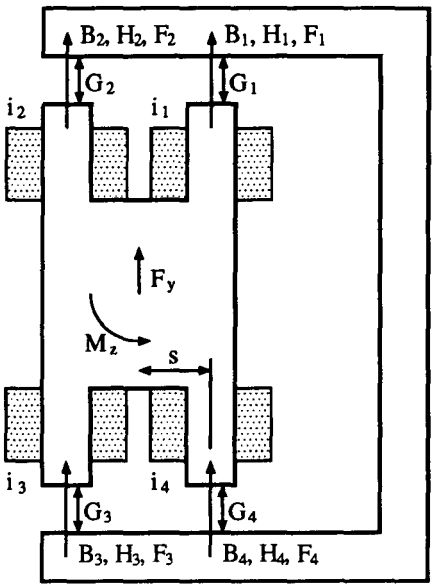

Figure 4: Schematic Cross Section of Magnetic Bearing

$$H_i = \frac{B_i}{\mu_0} \qquad i = 1, \ldots, 4 \tag{5}$$

$$\begin{Bmatrix} B_1 \\ B_2 \\ B_3 \\ B_4 \end{Bmatrix} = \frac{N\mu_0}{G_1G_2G_3 + G_1G_2G_4 + G_1G_3G_4 + G_2G_3G_4} \tag{6}$$

$$\begin{bmatrix} G_2G_3 + G_2G_4 \\ +G_3G_4 & -G_3G_4 & G_2G_4 & G_2G_3 \\ -G_3G_4 & G_1G_3 + G_1G_4 \\ & +G_3G_4 & G_1G_4 & G_1G_3 \\ G_2G_4 & G_1G_4 & G_1G_2 + G_1G_4 \\ & & +G_2G_4 & -G_1G_2 \\ G_2G_3 & G_1G_3 & -G_1G_2 & G_1G_2 + G_1G_3 \\ & & & +G_2G_3 \end{bmatrix} \begin{Bmatrix} i_1 \\ i_2 \\ i_3 \\ i_4 \end{Bmatrix}$$

The four gaps are geometrically related to the offset of the stator with respect to the flotor by the relations (7) which assume small angles.

$$\begin{aligned} G_1 &= G_0 - y - s\theta \\ G_2 &= G_0 - y + s\theta \\ G_3 &= G_0 + y - s\theta \\ G_4 &= G_0 + y + s\theta \end{aligned} \tag{7}$$

G_0 is the air gap length with the stator centered in the flotor.

The magnetic energy stored in the magnetic bearing (ω_m) is found from (8) where A_g is the area of the pole faces.

$$\begin{aligned}\omega_m &= \frac{1}{2}\int_{\infty} \underline{\mathrm{B}} \cdot \underline{\mathrm{H}}\, dV \\ &= \frac{A_g}{2\mu_0}\left(B_1^2 G_1 + B_2^2 G_2 + B_3^2 G_3 + B_4^2 G_4\right)\end{aligned} \tag{8}$$

The force and moment on the stator are found from the relations (9) and (10).

$$F_y = \frac{\partial \omega_m}{\partial y} \tag{9}$$

$$M_z = \frac{\partial \omega_m}{\partial \theta} \tag{10}$$

After considerable algebraic manipulation, and introduction (without loss of generality) of the linear current transformations (11) we obtain the force and moment relations sought (12) and (13).

$$\begin{aligned} j_1 &= i_1 + i_2 + i_3 + i_4 \\ j_2 &= i_1 - i_2 + i_3 - i_4 \\ j_3 &= i_1 - i_2 - i_3 + i_4 \end{aligned} \tag{11}$$

$$F_y = \frac{A_g N^2 \mu_0 \left(G_0 j_2 + \theta s j_1 + y j_3\right)\left(G_0^2 j_3 - \theta^2 s^2 j_3 + G_0 y j_2 + \theta s y j_1\right)}{4 G_0 \left(G_0^2 - \theta^2 s^2 - y^2\right)^2} \tag{12}$$

$$M_z = \frac{A_g N^2 s \mu_0 \left(G_0 j_2 + \theta s j_1 + y j_3\right)\left(G_0^2 j_1 + G_0 \theta s j_2 + \theta s y j_3 - y^2 j_1\right)}{4 G_0 \left(G_0^2 - \theta^2 s^2 - y^2\right)^2} \tag{13}$$

The current j_2 is analogous to the bias current in a conventional bidirectional thrust bearing and could be fixed at a constant value — nominally half of the maximum current. The force generated is predominantly driven by j_3 and the moment by j_1. The system is unstable (negative stiffness) in both translation and rotation. The currents $i_1, \ldots, i_4$ can be found by a pseudo-inverse technique from j_1, j_2, j_3. Closed form analytic inverses to (12) and (13) have been found for a known position.

4 Predicted Performance

The equations of the previous section were used to predict the performance of a specific design. The design has a center cube of 2 in. on a side, pole faces of 1 x .5 in., and pole length of 2 in. Maximum current is determined by allowing a coil current density of 5000 amp/in^2 which is known to be conservative from previous designs. The gap in the centered position was chosen to be .125 in. plus an allowance of .030 in. for inclusion of flux sensors and a protective layer on the inside of the bands. The resulting specifications for the design are presented in Table 2. The 53 N force is a continuous worst case, with the stator moved away from the flotor in the direction of the force. The continuous force capability in the centered position is 175 N. Intermittent force capability is limited only by the current capability of the amplifiers, and the saturation limit of the magnetic material used. Using Vanadium Permadur with this design, saturation would occur at about 1000 N. Of the 4.5 kg weight, the flotor comprises only 1.2 kg.

Trans.	*Rot.*	*Force*	*Envelope*	*Weight*
±3.2 mm	±7°	53 N	15x15x15 cm	4.5 kg

Table 2: Specification of UVA Design

When compared with the designs presented in Table 1, the UVA design has several advantages. The envelope is substantially smaller than any of the previous designs, while the performance is similar. In addition to saving space, this compactness allows the flotor to be naturally rigid, and thus avoids control problems with structural dynamics. The design is quite dense in comparison with the others, but it is lighter than the lightest for which data were available.

5 Control

A regulator has been designed to reject the disturbances caused by the umbilical connection to the experiment. A schematic is shown in Figure 5. Nonlinearities in the magnetic bearing are eliminated by using flux feedback in a minor loop [3]. Six accelerometers mounted on the flotor produce a generalized acceleration signal which is fed back through a linear controller. More details on the controller are available in [9]. The desired control force is processed through an inverse magnetic circuit model to obtain a desired flux signal. This model could be either a digital algebraic model, or an appropriately trained neural network.

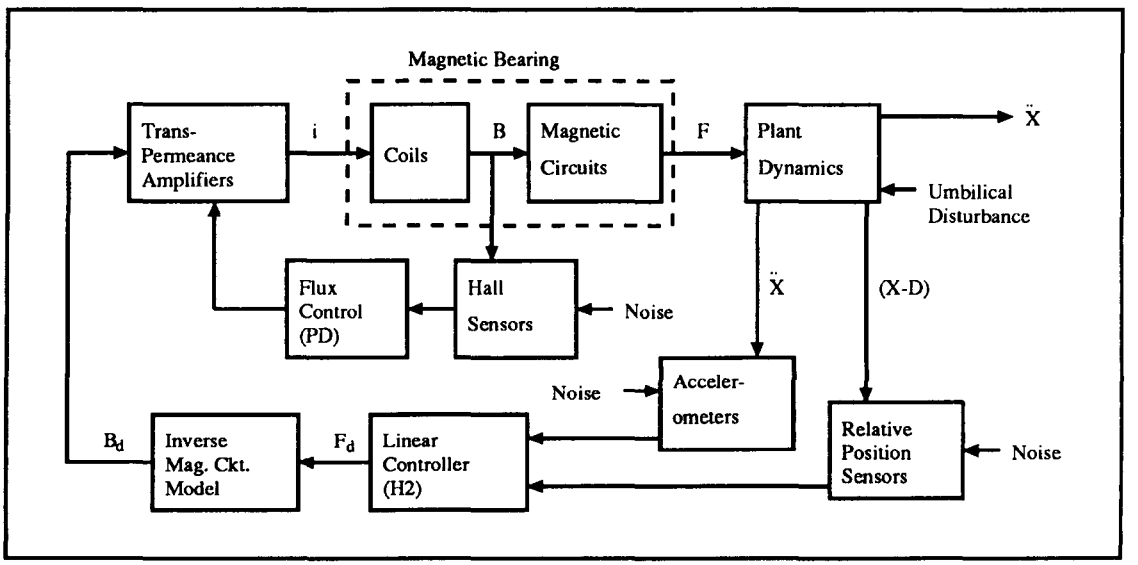

Figure 5: Control Schematic

A relative position sensor has not been chosen but the optical scheme used in IBM's design is a strong candidate. Alternatively, the current and flux signals could be processed to infer position [10]. The purpose of the relative position signal is only to prevent collision with the walls, so accuracy demands are relatively low.

6 Conclusion

A design for a novel magnetic bearing, proposed as the fine stage of a coarse-fine actuator for microgravity vibration isolation, has been presented. The bearing is novel in that it uses a geometry that has just three independent flux path systems. This contrasts the twelve flux path systems (six bidirectional thrust bearings) used in conventional designs. The novel design results in compactness, light weight and high performance, when compared with the published designs. A control system is proposed to reject disturbances caused by an umbilical connection to the experiment.

Future work will focus on building a laboratory version of the bearing and control system.

References

[1] A. Peter Allan and Carl R. Knospe. A six degree-of-freedom actuator design for microgravity vibration isolation. In *International Workshop on Vibration Isolation Technology for Microgravity Science Applications*, Cleveland, Ohio, April 23-25, 1991. NASA Lewis Research Center.

[2] D. Stewart. A platform with six degrees of freedom. *Proceedings of the Institute of Mechanical Engineers*, 180(1):371–386, 1965.

[3] Terry S. Allen, Douglas D. Havenhill, and Kevin D. Kral. FEAMIS: A magnetically suspended isolation system for space-based materials processing. In *Annual AAS Guidance and Control Conference*, Keystone, Colorado, February 1-5, 1986. Rocky Mountain Section, American Astronautical Society.

[4] D. I. Jones, A. R. Owens, and R. G. Owen. A microgravity isolation mount. *Acta Astronautica*, 15(6/7):441–448, 1987.

[5] Carlos M. Grodsinsky. Development and approach to low-frequency microgravity isolation systems. Technical Paper 2984, NASA, August 1990.

[6] Ralph Fenn and Bruce Johnson. A six degree of freedom Lorentz force vibration isolator with nonlinear controller. In *International Workshop on Vibration Isolation Technology for Microgravity Science Applications*, Cleveland, Ohio, April 23-25, 1991. NASA Lewis Research Center.

[7] Ralph L. Hollis, S. E. Salcudean, and A. Peter Allan. A six degree-of-freedom magnetically levitated variable compliance fine-motion wrist: Design, modeling and control. *IEEE Transactions on Robotics and Automation*, 7(3):320–332, 1991.

[8] Kenichi Takahara, Tamane Ozawa, Hiroshi Takahashi, Shitta Shingu, Toshiro Ohashi, and Hitoshi Sugiura. Development of a magnetically suspended, tetrahedron-shaped antenna pointing system. In *22nd Aerospace Mechanisms Symposium*, Hampton, VA, May 4-6, 1988. NASA Langley Research Center.

[9] R. D. Hampton and Carl R. Knospe. Extended H_2 synthesis for multiple-degree-of-freedom controllers. In *International Symposium on Magnetic Suspension Technology*, Hampton, VA, August 19-23, 1991. NASA Langley Research Center.

[10] D. Zlatnik and A. Traxler. Cost-effective implementation of active magnetic bearings. In *2nd International Symposium on Magnetic Bearings*, Tokyo, Japan, July 12-14, 1990. Institute of Industrial Science, University of Tokyo.